

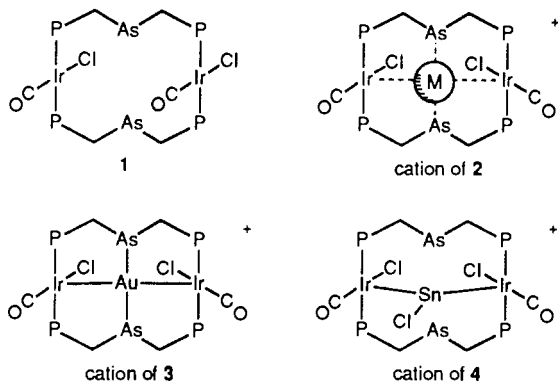
## Bonding of Sulfur Dioxide to the Metallamacrocyclic $\text{Ir}_2(\text{CO})_2\text{Cl}_2(\mu\text{-}(\text{Ph}_2\text{PCH}_2)_2\text{AsPh})_2$ and Its Gold(I) Adduct $[\text{Ir}_2\text{Au}(\text{CO})_2\text{Cl}_2(\mu\text{-}(\text{Ph}_2\text{PCH}_2)_2\text{AsPh})_2]^+$

Alan L. Balch,\* Brian J. Davis, and Marilyn M. Olmstead

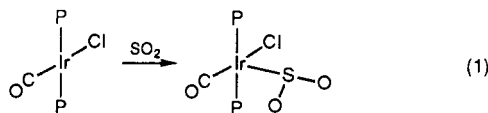
Received February 28, 1989

Treatment of a dichloromethane solution of  $\text{Ir}_2(\text{CO})_2\text{Cl}_2(\mu\text{-dpma})_2$  (dpma is bis(diphenylphosphino)methylphenylarsine) with sulfur dioxide produces the adduct  $\text{Ir}_2(\text{SO}_2)_2(\text{CO})_2\text{Cl}_2(\mu\text{-dpma})_2$ . Green needles of  $\text{Ir}_2(\text{SO}_2)_2(\text{CO})_2\text{Cl}_2(\mu\text{-dpma})_2 \cdot 3\text{CHCl}_3 \cdot 0.5\text{CH}_2\text{Cl}_2$  crystallized in the monoclinic space group  $P2_1/n$  (no. 14), with  $a = 14.699$  (4) Å,  $b = 15.351$  (6) Å,  $c = 38.026$  (10) Å,  $\beta = 100.03$  (3)°, and  $Z = 4$  at 130 K. Refinement of 11 045 reflections with 461 parameters yielded  $R = 0.078$  and  $R_w = 0.079$ . The adduct consists of one molecule of sulfur dioxide bonded through sulfur to each of the iridium atoms in the intact metallamacrocyclic. There is no interaction between the two iridium coordination spheres other than through the bridging phosphine ligands. The geometry of the roughly square-pyramidal  $\text{IrS}(\text{CO})\text{ClP}_2$  units is very similar to that found in  $\text{Ir}(\text{SO}_2)(\text{CO})\text{Cl}(\text{PPh}_3)_2$ . Addition of sulfur dioxide to  $[\text{Ir}_2\text{Au}(\text{CO})_2\text{Cl}_2(\mu\text{-dpma})_2]\text{Cl}$  in dichloromethane produces a red adduct that has been obtained in crystalline form on prolonged standing in a sulfur dioxide saturated dichloromethane/ether solution. Red  $[\text{Ir}_2\text{Au}(\text{SO}_2)_2(\text{CO})_2\text{Cl}_2(\mu\text{-dpma})_2][\text{HSO}_4] \cdot 0.32\text{SO}_2 \cdot 1.23\text{H}_2\text{O}$  crystallizes in the triclinic space group  $P1$  with  $a = 12.548$  (4) Å,  $b = 15.721$  (4) Å,  $c = 20.556$  (5) Å,  $\alpha = 76.97$  (2)°,  $\beta = 73.60$  (2)°,  $\gamma = 83.35$  (2)°, and  $Z = 2$  at 130 K. Refinement of 10 356 reflections with  $I > 2\sigma(I)$ , using 807 parameters, yielded  $R = 0.059$  and  $R_w = 0.065$ . The structure shows that the  $[\text{Ir}_2\text{Au}(\text{CO})_2\text{Cl}_2(\mu\text{-dpma})_2]^+$  undergoes only modest changes upon binding sulfur dioxide, which coordinates one of the iridium ions through sulfur. As a result, the gold atom is displaced closer to the iridium atom that is not bound to the sulfur dioxide ( $\text{Au}\cdots\text{Ir} = 2.953$  (1) Å) and further from the sulfur-bound iridium ( $\text{Au}\cdots\text{Ir} = 3.132$  (1) Å). Sulfur dioxide does not bind to  $[\text{Ir}_2(\text{SnCl})(\text{CO})_2\text{Cl}_2(\mu\text{-dpma})_2]^+$ .

The metallamacrocyclic  $\text{Ir}_2(\text{CO})_2\text{Cl}_2(\mu\text{-dpma})_2$  (**1**)<sup>1</sup> and its metal complexes (cation **2**)<sup>2,3</sup> are complicated substances with a variety of binding sites that are available for interaction with small Lewis acids or bases. Sulfur dioxide is an amphoteric substance capable of binding transition-metal complexes in a wide array of structural variants.<sup>4</sup> Here we explore its interaction with **1**, the gold(I) adduct (cation **3**), and the tin(II) adduct (cation **4**).



Sulfur dioxide is known to bind  $\text{Ir}(\text{CO})\text{Cl}(\text{PPh}_3)_2$  (Vaska's complex) through sulfur to give the roughly square-pyramidal  $\text{Ir}(\text{SO}_2)(\text{CO})\text{Cl}(\text{PPh}_3)_2$  (eq 1) with the  $\text{SO}_2$  plane inclined at an



- (1) (a) Balch, A. L.; Fossett, L. A.; Olmstead, M. M.; Oram, D. E.; Reedy, P. E., Jr. *J. Am. Chem. Soc.* **1985**, *107*, 5272. (b) Balch, A. L. *Pure Appl. Chem.* **1988**, *60*, 555.
- (2) (a) Balch, A. L.; Fossett, L. A.; Olmstead, M. M.; Reedy, P. E., Jr. *Organometallics* **1986**, *5*, 1929. (b) Balch, A. L.; Ghedini, M.; Oram, D. E.; Reedy, P. E., Jr. *Inorg. Chem.* **1987**, *26*, 1223. (c) Balch, A. L.; Oram, D. E.; Reedy, P. E., Jr. *Inorg. Chem.* **1987**, *26*, 1836. (d) Balch, A. L.; Nagle, J. K.; Olmstead, M. M.; Reedy, P. E., Jr. *J. Am. Chem. Soc.* **1987**, *109*, 4123. (e) Balch, A. L.; Fossett, L. A.; Olmstead, M. M.; Reedy, P. E., Jr. *Organometallics* **1988**, *7*, 430. (f) Balch, A. L.; Olmstead, M. M.; Neve, F.; Ghedini, M. *New J. Chem.* **1988**, *12*, 529. (g) Balch, A. L.; Olmstead, M. M.; Oram, D. E.; Reedy, P. E., Jr.; Reimer, S. H. *J. Am. Chem. Soc.* **1989**, *111*, 4021.
- (3) Balch, A. L.; Nagle, J. K.; Oram, D. E.; Reedy, P. E., Jr. *J. Am. Chem. Soc.* **1988**, *110*, 454.
- (4) Ryan, R. R.; Kubas, G. J.; Moody, D. C.; Eller, P. G. *Struct. Bonding* **1981**, *46*, 47. Mingos, D. M. P. *Transition Met. Chem. (Weinheim, Ger.)* **1978**, *3*, 1.

angle of 121.6° to the Ir-S bond.<sup>5,6</sup> While similar behavior might be anticipated for **1**, **3**, and **4**, the ability of **1** to bind Lewis acids with an  $s^2$  electronic configuration (e.g. Sn(II), Pb(II), Tl(I)) through an Ir-M-Ir structure<sup>2d,8</sup> and the proximity of the metal ions to both iridium atoms in **3** and **4** might be expected to have important consequences on the structures of any adducts with sulfur dioxide formed by **1**, **3**, and **4**.

### Results

**Addition of Sulfur Dioxide to  $\text{Ir}_2(\text{CO})_2\text{Cl}_2(\mu\text{-dpma})_2$  (**1**).** Treatment of a yellow dichloromethane or chloroform solution of **1** with sulfur dioxide results in a color change to light yellow-green. The 81-MHz <sup>31</sup>P NMR spectrum of the chloroform solution shows a change from the singlet at 18.5 ppm to a new singlet at 3.8 ppm for the adduct **5**. The infrared spectrum of the solution shows the expected increase of  $\nu(\text{CO})$  from 1967  $\text{cm}^{-1}$  for **1** to 2025  $\text{cm}^{-1}$  for the adduct, and the optical spectrum shows the characteristic three band pattern of **1** at 336, 383, and 432  $\text{nm}^{-1}$  changed to a single broad absorbance with  $\lambda_{\text{max}} = 410$  nm ( $\epsilon = 30\,400$ ) for the adduct.

Crystals of the adduct **5** suitable for X-ray diffraction were obtained by diffusion of ether into a dichloromethane solution of **1** that had been saturated with sulfur dioxide. These crystals contain the same adduct as seen in solution. The infrared spectrum shows  $\nu(\text{CO})$  at 2023 and 2015  $\text{cm}^{-1}$  and bands due to coordinated sulfur dioxide at 1184 and 1041  $\text{cm}^{-1}$ . However, the crystals are unstable to sulfur dioxide loss. When the light green crystals are stored under vacuum for 12 h, they become yellow, and the infrared bands due to the coordinated sulfur dioxide disappear and  $\nu(\text{CO})$  moves to 1962  $\text{cm}^{-1}$ .

Figure 1 shows a perspective view of the molecule obtained from the X-ray diffraction study. Atomic coordinates are given in Table I. The macrocyclic structure has remained intact while one sulfur dioxide has bound to each iridium in the same fashion as seen for Vaska's complex (eq 1). Selected interatomic distances are given in Table II where they can be compared to the corresponding distances in both  $\text{Ir}(\text{SO}_2)(\text{CO})\text{Cl}(\text{PPh}_3)_2$ <sup>6</sup> and  $\text{Rh}(\text{SO}_2)(\text{CO})\text{Cl}(\text{PPh}_3)_2$ .<sup>7</sup> Selected interatomic angles are collected and compared in Table III.

The coordination geometry in the vicinity of both iridium atoms of **5** is similar with respect to both bond distances and angles. Moreover, the metal ion geometry is similar to that seen in the mononuclear complexes  $\text{M}(\text{CO})\text{Cl}(\text{PPh}_3)_2$  ( $\text{M} = \text{Rh}, \text{Ir}$ ). In all

(5) Vaska, L. *Acc. Chem. Res.* **1968**, *1*, 335.

(6) La Placa, S. J.; Ibers, J. A. *Inorg. Chem.* **1966**, *5*, 405.

(7) Muir, K. W.; Ibers, J. A. *Inorg. Chem.* **1969**, *8*, 1921.

**Table I.** Atomic Coordinates ( $\times 10^4$ ) and Isotropic Thermal Parameters ( $\text{\AA}^2 \times 10^3$ ) for Ir<sub>2</sub>Cl<sub>2</sub>(CO)<sub>2</sub>(SO<sub>2</sub>)<sub>2</sub>( $\mu$ -dpma)<sub>2</sub>

	<i>x</i>	<i>y</i>	<i>z</i>	<i>U</i>		<i>x</i>	<i>y</i>	<i>z</i>	<i>U</i>
Ir(1)	2198 (1)	6034 (1)	6070 (1)	19 (1) <sup>a</sup>	C(33)	-3626 (28)	4603 (31)	5409 (11)	47 (12)
Ir(2)	-1353 (1)	5391 (1)	6686 (1)	17 (1) <sup>a</sup>	C(34)	-2883 (29)	4499 (30)	5643 (11)	46 (13)
As(1)	300 (3)	4437 (3)	6371 (1)	22 (1) <sup>a</sup>	C(35)	-6 (26)	6353 (27)	7394 (10)	34 (11)
As(2)	1404 (3)	7643 (3)	6922 (1)	25 (2) <sup>a</sup>	C(36)	939 (24)	6019 (28)	7440 (10)	32 (10)
Cl(1)	2139 (6)	5671 (6)	6667 (2)	22 (3) <sup>a</sup>	C(37)	1367 (33)	5721 (30)	7796 (12)	55 (14)
Cl(2)	-1653 (6)	6184 (7)	6142 (2)	25 (4) <sup>a</sup>	C(38)	876 (31)	5687 (31)	8052 (13)	57 (15)
S(1)	582 (7)	6310 (7)	5851 (3)	25 (4) <sup>a</sup>	C(39)	-121 (27)	5952 (29)	8011 (11)	39 (12)
S(2)	-2789 (7)	5699 (7)	6893 (3)	27 (4) <sup>a</sup>	C(40)	-456 (23)	6247 (23)	7693 (8)	17 (9)
P(1)	2104 (7)	4513 (8)	5966 (2)	24 (4) <sup>a</sup>	C(41)	-1309 (22)	7547 (24)	7048 (9)	15 (9)
P(2)	-1821 (6)	4151 (7)	6338 (3)	18 (4) <sup>a</sup>	C(42)	-2064 (22)	7731 (24)	6791 (9)	17 (9)
P(3)	-586 (7)	6628 (7)	6968 (3)	23 (4) <sup>a</sup>	C(43)	-2652 (23)	8434 (23)	6831 (9)	16 (9)
P(4)	2537 (7)	7462 (7)	6256 (3)	23 (4) <sup>a</sup>	C(44)	-2408 (26)	8974 (30)	7119 (10)	36 (11)
O(1)	2679 (21)	6386 (22)	5359 (8)	65 (10)	C(45)	-1624 (28)	8834 (31)	7373 (11)	49 (13)
O(2)	-756 (17)	4356 (17)	7354 (7)	36 (8)	C(46)	-1118 (25)	8107 (25)	7322 (10)	26 (10)
O(3)	254 (16)	5674 (16)	5598 (6)	29 (7)	C(47)	274 (20)	6958 (23)	6713 (8)	9 (8)
O(4)	483 (17)	7186 (18)	5739 (7)	39 (8)	C(48)	835 (22)	8755 (23)	7037 (9)	14 (9)
O(5)	-2525 (17)	5878 (18)	7283 (7)	35 (7)	C(49)	232 (28)	9222 (28)	6812 (12)	44 (13)
O(6)	-3353 (17)	4930 (18)	6804 (7)	37 (8)	C(50)	-170 (29)	9966 (29)	6918 (11)	42 (12)
C(1)	2462 (25)	6276 (26)	5620 (10)	27 (10)	C(51)	117 (27)	10262 (31)	7247 (11)	43 (12)
C(2)	-975 (25)	4711 (29)	7099 (10)	32 (11)	C(52)	803 (25)	9830 (27)	7502 (10)	34 (11)
C(3)	3028 (24)	3978 (28)	6290 (9)	28 (10)	C(53)	1118 (25)	9082 (28)	7382 (10)	31 (10)
C(4)	3879 (25)	4433 (29)	6335 (10)	36 (11)	C(54)	1671 (23)	8067 (25)	6455 (9)	19 (9)
C(5)	4648 (29)	4046 (30)	6574 (11)	45 (12)	C(55)	2801 (26)	8165 (28)	5928 (10)	31 (11)
C(6)	4507 (28)	3336 (28)	6762 (11)	38 (12)	C(56)	1991 (31)	8616 (31)	5696 (11)	53 (14)
C(7)	3613 (28)	2943 (28)	6704 (11)	37 (11)	C(57)	2184 (39)	9099 (38)	5395 (15)	86 (19)
C(8)	2901 (27)	3212 (27)	6476 (10)	30 (11)	C(58)	3135 (32)	9175 (34)	5342 (13)	65 (16)
C(9)	2274 (21)	4095 (24)	5521 (8)	12 (8)	C(59)	3880 (33)	8803 (33)	5557 (12)	61 (15)
C(10)	2952 (26)	3509 (27)	5504 (10)	32 (11)	C(60)	3674 (36)	8290 (37)	5821 (14)	76 (18)
C(11)	3041 (24)	3233 (25)	5170 (9)	21 (10)	C(61)	3596 (24)	7492 (27)	6583 (9)	25 (10)
C(12)	2430 (26)	3437 (28)	4864 (11)	35 (11)	C(62)	3889 (33)	8356 (37)	6704 (13)	68 (16)
C(13)	1713 (25)	4044 (27)	4911 (10)	30 (10)	C(63)	4793 (25)	8374 (28)	6952 (10)	31 (11)
C(14)	1664 (25)	4404 (26)	5222 (9)	27 (10)	C(64)	5312 (29)	7660 (29)	7085 (11)	45 (13)
C(15)	1031 (21)	4017 (26)	6003 (8)	18 (9)	C(65)	4929 (23)	6842 (26)	6955 (9)	21 (10)
C(16)	700 (21)	3506 (24)	6711 (8)	11 (8)	C(66)	4105 (25)	6724 (29)	6711 (10)	33 (11)
C(17)	1119 (21)	3797 (25)	7060 (8)	18 (9)	Cl(3)	3032 (12)	6076 (13)	233 (5)	113 (6)
C(18)	1468 (25)	3117 (27)	7325 (11)	32 (11)	Cl(4)	3593 (14)	6364 (14)	971 (5)	130 (7)
C(19)	1370 (23)	2320 (26)	7235 (9)	24 (10)	Cl(5)	4706 (16)	5346 (17)	621 (6)	164 (9)
C(20)	954 (26)	2058 (30)	6895 (10)	39 (12)	C(67)	3961 (32)	6292 (35)	596 (12)	66 (16)
C(21)	640 (25)	2661 (28)	6653 (10)	31 (11)	Cl(6)	19 (11)	8400 (11)	403 (4)	89 (5)
C(22)	-832 (24)	3950 (31)	6094 (10)	38 (11)	Cl(7)	543 (11)	8608 (12)	1145 (4)	100 (6)
C(23)	-1970 (25)	3108 (27)	6578 (10)	28 (11)	Cl(8)	1303 (11)	7238 (11)	796 (4)	94 (5)
C(24)	-1914 (31)	2392 (34)	6387 (13)	59 (15)	C(68)	958 (36)	8262 (37)	760 (13)	73 (17)
C(25)	-2017 (26)	1565 (29)	6553 (10)	34 (11)	Cl(9)	114 (22)	3703 (22)	313 (7)	105 (11)
C(26)	-2257 (33)	1581 (36)	6878 (13)	67 (16)	Cl(10)	-251 (27)	3406 (28)	1002 (8)	150 (16)
C(27)	-2280 (30)	2311 (31)	7074 (13)	58 (15)	Cl(11)	1042 (32)	4671 (30)	896 (11)	198 (22)
C(28)	-2177 (23)	3076 (26)	6904 (9)	20 (10)	Cl(12)	4287 (23)	1404 (23)	171 (9)	108 (12)
C(29)	-2857 (26)	4223 (26)	5979 (10)	28 (11)	Cl(13)	3003 (34)	2597 (34)	327 (14)	202 (23)
C(30)	-3652 (32)	3800 (33)	6073 (13)	64 (15)	Cl(14)	6869 (24)	4465 (25)	1334 (9)	126 (14)
C(31)	-4440 (30)	3869 (31)	5819 (11)	47 (13)	Cl(15)	6375 (26)	3444 (29)	731 (10)	156 (17)
C(32)	-4415 (35)	4229 (33)	5458 (14)	68 (16)	Cl(16)	8239 (24)	3881 (34)	964 (12)	177 (19)

<sup>a</sup> Equivalent isotropic *U* defined as one-third of the trace of the orthogonalized *U<sub>ij</sub>* tensor.

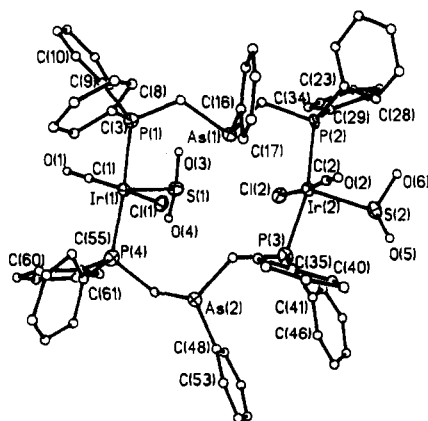


**Figure 1.** Perspective view of Ir<sub>2</sub>(SO<sub>2</sub>)<sub>2</sub>(CO)<sub>2</sub>Cl<sub>2</sub>( $\mu$ -dpma)<sub>2</sub> (**5**), showing the atomic numbering.

cases the iridium atom lies well out of the SO<sub>2</sub> plane. At Ir(1) the angle between the Ir-S bond and the SO<sub>2</sub> plane is 37.0° while at Ir(2) the corresponding angle is 29.4°.

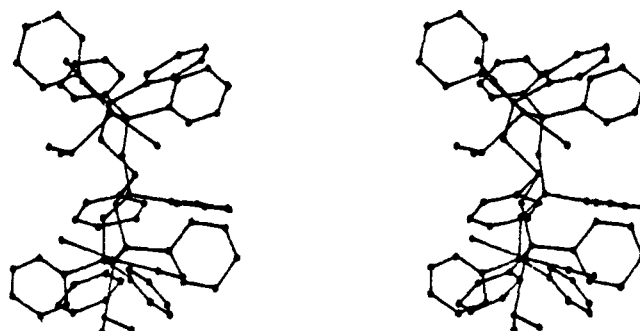


**Figure 2.** Stereoscopic drawing of Ir<sub>2</sub>(SO<sub>2</sub>)<sub>2</sub>(CO)<sub>2</sub>Cl<sub>2</sub>( $\mu$ -dpma)<sub>2</sub> (**5**), showing the relationship between the macrocyclic structure and the bound sulfur dioxide.

The relationship between the disposition of the macrocycle and the geometry of each iridium coordination environment is best seen in the stereoscopic view shown in Figure 2. Aside from the two bridging dpma ligands, there are no significant contacts between the two metal centers. The closest contact between the ligands on the two iridium atoms involves the S(1)···Cl(2) sepa-

**Table II.** Selected Interatomic Distances (Å)

	M(SO <sub>2</sub> )(CO)- Cl(PPh <sub>3</sub> ) <sub>2</sub>	5	6	3
		At Ir(1)		
Ir(1)-S(1)	2.488 (10) <sup>a</sup>	2.413 (9)	2.526 (3)	2.359 (9) <sup>c</sup>
Ir(1)-P(1)	2.359 (9) <sup>a</sup>	2.369 (12)	2.374 (3)	
Ir(1)-P(4)	2.328 (8) <sup>a</sup>	2.331 (11)	2.366 (3)	2.312 (4) <sup>c</sup>
Ir(1)-Cl(1)	2.371 (10) <sup>a</sup>	2.354 (9)	2.372 (3)	2.355 (4) <sup>c</sup>
Ir(1)-C(1)	1.96 (4) <sup>a</sup>	1.85 (4)	1.85 (1)	1.79 (2) <sup>c</sup>
Ir(1)-Au			3.132 (1)	3.059 (1) <sup>c</sup>
		At Ir(2)		
Ir(2)-S(2)	2.450 (2) <sup>b</sup>	2.426 (11)	2.325 (4)	2.324 (3) <sup>c</sup>
Ir(2)-P(2)	2.371 (2) <sup>b</sup>	2.351 (10)	2.325 (4)	2.324 (3) <sup>c</sup>
Ir(2)-P(3)	2.367 (2) <sup>b</sup>	2.369 (11)	2.330 (3)	2.317 (3) <sup>c</sup>
Ir(2)-Cl(2)	2.355 (2) <sup>b</sup>	2.374 (9)	2.377 (4)	2.357 (4) <sup>c</sup>
Ir(2)-C(2)	1.847 (7) <sup>b</sup>	1.89 (4)	1.85 (2)	1.81 (1) <sup>c</sup>
Ir(2)-Au			2.953 (1)	3.012 (1) <sup>c</sup>
		At Au		
Au-As(1)			2.388 (1)	2.397 (1) <sup>c</sup>
Au-As(2)			2.400 (1)	2.397 (1) <sup>c</sup>
Au-Ir(1)			3.132 (1)	3.059 (1) <sup>c</sup>
Au-Ir(2)			2.953 (1)	3.012 (1) <sup>c</sup>

<sup>a</sup>M = Ir. Data from ref 6. <sup>b</sup>M = Rh. Data from ref 6; read Rh for Ir(2). <sup>c</sup>Data from ref 3.

ration (3.649 (3) Å). Notice that this is significantly longer than the S-I distance of 3.391 Å in Pt(CH<sub>3</sub>)(PPh<sub>3</sub>)<sub>2</sub>I(SO<sub>2</sub>) where the sulfur dioxide is bound to the iodide rather than to the metal atom.<sup>8</sup> The sulfur dioxide moiety attached to Ir(2) is clearly situated on the outside of the macrocycle's cavity while the other sulfur dioxide is positioned somewhat to the side of the center. Binding of sulfur dioxide to Ir(1) appears to have caused rotation of the Cl-Ir-CO group about the P(1)-Ir(1)-P(4) axis since the orientation of that Cl-Ir-CO group (roughly trans to the Cl-Ir(2)-CO group) is different from that present in the parent macrocycle.<sup>2b</sup>

**Addition of Sulfur Dioxide to [Ir<sub>2</sub>Au(CO)<sub>2</sub>Cl<sub>2</sub>(μ-dpma)<sub>2</sub>]Cl (3).** When sulfur dioxide is added to a red dichloromethane or chloroform solution of **3**, there is a slight color change. The intense absorption feature at 508 nm (ε = 29 500) in **3** is shifted to 518 nm with a slight increase in intensity (ε = 31 600). The adduct **6** appears to be weakly emissive. The emission spectrum with 515-nm excitation shows a maximum at 609 nm in the presence of sulfur dioxide where as **3** alone shows an emission maximum at 604-nm. The intensity of the emission is about 0.06 that of **3**. The 81-MHz <sup>31</sup>P NMR spectrum of the resulting solution clearly shows that a reaction has occurred. In chloroform, the singlet at 15.6 ppm due to **3** is shifted to 5.8 ppm (at -60 °C) upon addition of sulfur dioxide. The spectrum of **6** is strongly temperature dependent. The resonance shifts to lower field on raising the temperature until at 25 °C it is at 9.9 ppm. However, at all temperatures the resonance is a singlet. No splitting into the two lines that would be expected on the basis of the crystal structure (vide infra) of the adduct is seen. We suspect that this is due to rapid exchange of sulfur dioxide between the two iridium ends of the cation. This process may easily be facilitated by the excess of free sulfur dioxide that is present.

Infrared spectroscopy of the solution also shows that an adduct forms. Compound **3** shows a carbon monoxide stretching band at 1971 cm<sup>-1</sup> in dichloromethane. After addition of sulfur dioxide to a dichloromethane solution of **3**, new bands at 2016 and 1974 cm<sup>-1</sup> are observed in the spectrum. These are consistent with the formation of an adduct with one sulfur dioxide bound to **3**. The carbon monoxide bound to the iridium which has sulfur dioxide added shows the expected increase in ν(CO) (to 2016 cm<sup>-1</sup>) while the carbon monoxide bound to the other iridium experiences a slight increase in ν(CO) (to 1974 cm<sup>-1</sup>).

Crystals of **6** have been isolated by layering a sulfur dioxide saturated dichloromethane solution of the adduct with diethyl ether. Crystal growth is a slow process. This is no doubt associated

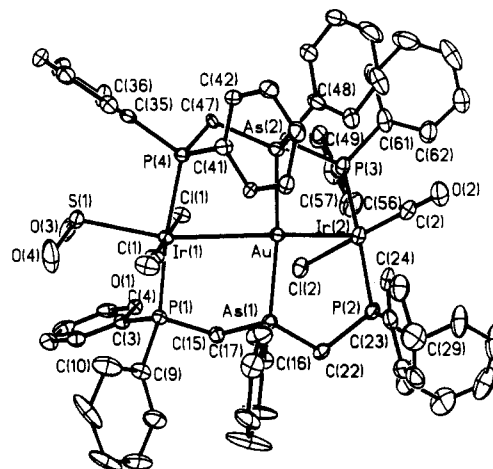


**Figure 3.** Perspective drawing of [Ir<sub>2</sub>Au(SO<sub>2</sub>)(CO)<sub>2</sub>Cl<sub>2</sub>(μ-dpma)<sub>2</sub>]<sup>+</sup> (cation **6**) with the atomic numbering.

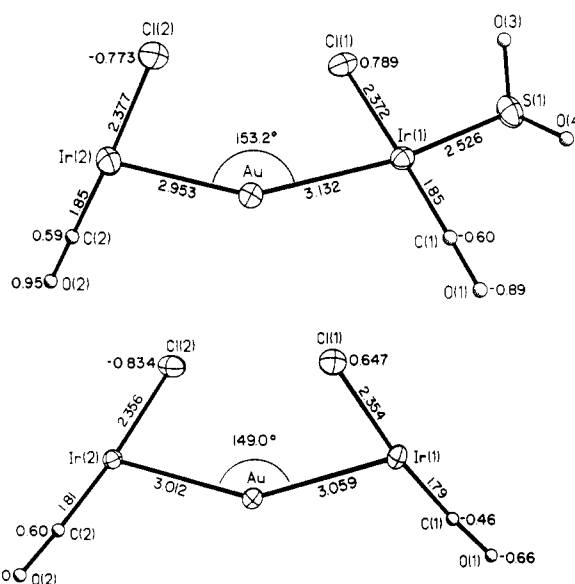


**Figure 4.** Comparison of the core portion of (top) [Ir<sub>2</sub>Au(SO<sub>2</sub>)(CO)<sub>2</sub>Cl<sub>2</sub>(μ-dpma)<sub>2</sub>]<sup>+</sup> (cation **6**) and (bottom) [Ir<sub>2</sub>Au(CO)<sub>2</sub>Cl<sub>2</sub>(μ-dpma)<sub>2</sub>]<sup>+</sup> (cation **3**), showing the structural changes accompanying sulfur dioxide bonding. Out-of-AuIr<sub>2</sub>-plane displacements (in Å) are given for the chloride and carbonyl ligands.

with the formation of the bisulfate anion that is found in the crystalline solid. Apparently the chloride salt does not form suitable crystals. However, after prolonged standing, sufficient bisulfate is formed by oxidation of sulfur dioxide (by adventitious dioxygen) so that the bisulfate salt crystallizes. The infrared spectrum of this salt shows ν(CO) at 2011 and 1959 cm<sup>-1</sup>, which is consistent with the observations made on the adduct in solution. Additionally, bands due to coordinated sulfur dioxide and bisulfite are present at 1224 (very broad) and 1043 cm<sup>-1</sup>, and broad bands due to water are observed at 3500 and 1633 cm<sup>-1</sup>.

A perspective drawing of the cation of **6** is shown in Figure 3. Atomic positional parameters are given in Table IV. The sulfur dioxide has added to one of the iridium ions within the complex cation in the usual pyramidal fashion. Selected structural parameters are collected in Tables II and III where they can be compared to corresponding values for the other sulfur dioxide adducts and for the gold/iridium complex **3**.

Further comparison of **3** and its sulfur dioxide adduct **6** can be made by turning to Figure 4, which shows comparable sections of the two cations. These views look down on the IrAuIr portion and leave out the bridging phosphine ligands. However, the ligands shown in this view for both **3** and **6** do not lie in a common plane. The Cl-Ir-Cl units are each twisted out of the plane, and for **6**, the SO<sub>2</sub> unit is bent out of the plane as well. The major difference

(8) Snow, M. R.; McDonald, J.; Basolo, F.; Ibers, J. A. *J. Am. Chem. Soc.* **1972**, *94*, 2527.

Table III. Selected Interatomic Angles (deg)

	M(SO <sub>2</sub> )(CO)- Cl(PPh <sub>3</sub> ) <sub>2</sub>		
	5	6	3
At Ir(1)			
S(1)-Ir(1)-Cl(1)	97.4 (3) <sup>a</sup>	100.1 (3)	93.6 (1)
S(1)-Ir(1)-P(1)	92.6 (4) <sup>a</sup>	95.2 (3)	94.7 (1)
S(1)-Ir(1)-P(3)	97.8 (4) <sup>a</sup>	94.9 (3)	91.1 (1)
S(1)-Ir(1)-C(1)	89.8 (1.1) <sup>a</sup>	89.9 (1.1)	87.9 (4)
Au-Ir(1)-Cl(1)			73.1 (1)
Au-Ir(1)-P(1)			93.7 (1)
Au-Ir(1)-P(3)			79.6 (1)
Au-Ir(1)-C(1)			105.2 (4)
Cl(1)-Ir(1)-P(1)	87.3 (4) <sup>a</sup>	85.3 (3)	85.5 (1)
Cl(1)-Ir(1)-P(3)	89.3 (3) <sup>a</sup>	88.4 (3)	89.6 (1)
C(1)-Ir(1)-P(1)	92.8 (1.0) <sup>a</sup>	93.3 (1.3)	95.3 (3)
C(1)-Ir(1)-P(3)	89.4 (1.0) <sup>a</sup>	91.4 (1.2)	89.5 (3)
S(1)-Ir(1)-Au			163.7 (1)
P(1)-Ir(1)-P(3)	169.5 (4) <sup>a</sup>	168.9 (3)	172.6 (1)
Cl(1)-Ir(1)-C(1)	172.8 (1.0) <sup>a</sup>	170.0 (1.1)	178.3 (4)
At Ir(2)			
S(2)-Ir(2)-Cl(2)	99.4 (1) <sup>b</sup>	98.2 (3)	
S(2)-Ir(2)-P(2)	93.6 (1) <sup>b</sup>	98.9 (3)	
S(2)-Ir(2)-P(4)	98.7 (1) <sup>b</sup>	93.9 (4)	
S(2)-Ir(2)-C(2)	89.6 (2) <sup>b</sup>	89.0 (1.2)	
Au-Ir(2)-Cl(2)			77.5 (1)
Au-Ir(2)-P(2)			83.5 (1)
Au-Ir(2)-P(4)			96.8 (1)
Au-Ir(2)-C(2)			105.1 (4)
Cl(2)-Ir(2)-P(2)	86.6 (1) <sup>b</sup>	86.2 (3)	88.8 (1)
Cl(2)-Ir(2)-P(4)	89.2 (1) <sup>b</sup>	89.2 (3)	87.2 (1)
C(2)-Ir(2)-P(2)	91.7 (2) <sup>b</sup>	92.0 (1.3)	91.4 (4)
C(2)-Ir(2)-P(4)	90.6 (2) <sup>b</sup>	91.0 (1.2)	92.5 (4)
P(2)-Ir(2)-P(4)	167.6 (1) <sup>b</sup>	166.9 (4)	175.8 (1)
Cl(2)-Ir(2)-C(2)	170.9 (2) <sup>b</sup>	172.7 (1.3)	177.4 (4)
At Au			
Ir(1)-Au-As(1)			83.4 (1)
Ir(1)-Au-As(2)			92.6 (1)
Ir(2)-Au-As(1)			93.9 (1)
Ir(2)-Au-As(2)			85.2 (1)
Ir(1)-Au-Ir(2)			153.2 (1)
As(1)-Au-As(2)			169.3 (1)
At S(1)			
Ir(1)-S(1)-O(3)	104.2 (1.5) <sup>a</sup>	108.4 (1.1)	104.6 (4)
Ir(1)-S(1)-O(4)	107.6 (1.5) <sup>a</sup>	108.3 (1.1)	104.5 (5)
O(3)-S(1)-O(4)	117.1 (1.5) <sup>a</sup>	116.9 (1.5)	111.7 (9)
At S(2)			
Ir(2)-S(2)-O(5)	105.3 (2) <sup>b</sup>	105.6 (1.1)	
Ir(2)-S(2)-O(6)	106.7 (2) <sup>b</sup>	105.1 (1.2)	
O(5)-S(2)-O(6)	113.8 (3) <sup>b</sup>	115.0 (1.6)	

<sup>a</sup> M = Ir. Data from ref 6. <sup>b</sup> M = Rh. Data from ref 6; read Rh for Ir(2). <sup>c</sup> Data from ref 3.

between the macrocyclic core of **3** and **6** involves the placement of the gold atom. In **6** it is displaced away from Ir(1) toward Ir(2) so that its coordination environment is decidedly asymmetric. However, the As-Au distances in both structures are similar and the Ir-Au-Ir angle in **6** is only 3° greater in **6** than that in **3**. Bond distances and angles both at Ir(1) and Ir(2) are similar to those in **3**.

The sulfur dioxide is bound to Ir(1) in the pyramidal fashion seen in Ir(SO<sub>2</sub>)(CO)Cl(PPh<sub>3</sub>)<sub>2</sub> and in **2**. However, the Ir-S bond in **6** (2.526 (3) Å) is significantly longer than the Ir-S bonds in **3** or in Ir(SO<sub>2</sub>)(CO)Cl(PPh<sub>3</sub>)<sub>2</sub>. The mutual lengthening of the Ir-Au and Ir-S distances in **6** can be attributed to the trans effects by each of these ligands.

**Attempted Addition of Sulfur Dioxide to [Ir<sub>2</sub>(SnCl)(CO)<sub>2</sub>Cl<sub>2</sub>(μ-dpma)<sub>2</sub>]BPh<sub>4</sub> (**4**).** When **4** is treated with sulfur dioxide under conditions comparable to those used for the formation of **5** and **6**, the tin complex **4** remains unchanged as shown by the electronic spectrum and the emission spectrum, which are not altered.

## Discussion

The structural studies presented here indicate the sulfur dioxide binds the iridium ions in the metallamacrocyclic **1** and its gold(I)

adduct **3** in the same fashion as it does the simpler mononuclear complex Ir(CO)Cl(PPh<sub>3</sub>)<sub>2</sub>. Studies of other metallamacrocyclics have shown that these readily add one small molecule but that addition of a second can be difficult. For example, Rh<sub>2</sub>(CO)<sub>2</sub>Cl<sub>2</sub>(μ-Ph<sub>2</sub>P(CH<sub>2</sub>)<sub>3</sub>PPh<sub>2</sub>)<sub>2</sub> readily adds one sulfur dioxide under conditions where **5** is formed, but no evidence for the uptake of a second molecule of sulfur dioxide was observed.<sup>9</sup> Similarly, Ir<sub>2</sub>(CO)<sub>2</sub>Cl<sub>2</sub>(μ-Ph<sub>2</sub>P(CH<sub>2</sub>)<sub>3</sub>PPh<sub>2</sub>)<sub>2</sub> reacts under 1 atm of dioxygen to form the monoadduct, Ir<sub>2</sub>(O<sub>2</sub>)(CO)<sub>2</sub>Cl<sub>2</sub>(μ-Ph<sub>2</sub>P(CH<sub>2</sub>)<sub>3</sub>PPh<sub>2</sub>)<sub>2</sub>.<sup>10</sup> However, at higher dioxygen pressure, the bisadduct, Ir<sub>2</sub>(O<sub>2</sub>)<sub>2</sub>(CO)<sub>2</sub>Cl<sub>2</sub>(μ-Ph<sub>2</sub>P(CH<sub>2</sub>)<sub>3</sub>PPh<sub>2</sub>)<sub>2</sub>, forms. Interestingly, **1** does not form a dioxygen adduct under 1 atm of dioxygen. Ir<sub>2</sub>(CO)<sub>2</sub>Cl<sub>2</sub>(μ-Ph<sub>2</sub>P(CH<sub>2</sub>)<sub>3</sub>PPh<sub>2</sub>)<sub>2</sub> reacts with dihydrogen at 1 atm to yield a mixture of di- and tetrahydrido species with the formation of the tetrahydride incomplete at 3 atm.<sup>10</sup> In the case of the formation of **5**, however, while the addition is no doubt stepwise, there is no problem in isolating the adduct with sulfur dioxide bound to both iridium atoms.

In **5**, the sulfur dioxide molecules are bound to the side of the metallamacrocyclic, and the interior cavity remains relatively empty as seen in Figure 2. The arsenic atoms do not appear to interact with the added sulfur dioxide ligands. In Ir<sub>2</sub>(O<sub>2</sub>)(CO)<sub>2</sub>Cl<sub>2</sub>(μ-Ph<sub>2</sub>P(CH<sub>2</sub>)<sub>3</sub>PPh<sub>2</sub>)<sub>2</sub> the dioxygen ligand also lies to the side of the macrocycle and the interior is relatively empty.<sup>10</sup> However, in both Ir<sub>2</sub>(H)<sub>2</sub>(CO)<sub>2</sub>Cl<sub>2</sub>(μ-Ph<sub>2</sub>P(CH<sub>2</sub>)<sub>3</sub>PPh<sub>2</sub>)<sub>2</sub> and Ir<sub>2</sub>(H)<sub>4</sub>(CO)<sub>2</sub>Cl<sub>2</sub>(μ-Ph<sub>2</sub>P(CH<sub>2</sub>)<sub>3</sub>PPh<sub>2</sub>)<sub>2</sub>, the hydride ligands lie in the interior of the macrocycle.<sup>10</sup>

The presence of the gold ion within the macrocyclic cavity does not exclude sulfur dioxide binding. Although vacant coordinate sites are present at both gold (with four neighboring atoms) and iridium (with five neighboring atoms), it is one of the iridium centers that is capable of bonding to sulfur dioxide. This reactivity parallels that seen with halogens which react with **3** by three-center oxidative addition that results in halogen atom addition to each iridium without altering the coordination number of gold but with a significant reduction in the gold-iridium distances.<sup>3</sup>

However, the structural change seen in Figure 4 contrasts with the observations of Fackler and co-workers<sup>11</sup> regarding sulfur dioxide addition to a binuclear Au(I) complex and a Au<sub>2</sub>Pt<sup>II</sup> chain. In both cases they observed addition of two sulfur dioxide molecules to the complexes to give O<sub>2</sub>SAuAuSO<sub>2</sub> and O<sub>2</sub>SAuPtAuSO<sub>2</sub> units in which the Au-Au and Au-Pt distances are shortened in comparison with those of their sulfur dioxide free precursors. They interpreted this shortening to partial oxidation of the bi- or trinuclear unit. While oxidation addition of halogens to **3** results in appreciable shortening of the Au-Ir distances, the unsymmetrical addition of sulfur dioxide results in the modest shift of the gold ion away from Ir(1). It appears that the binding of sulfur dioxide asymmetrically in **3** results in isolation of one Ir(CO)ClP<sub>2</sub> unit (which itself is fully capable of adding sulfur dioxide) from the Ir-Au-Ir chain. It would be interesting to see the structural effects of addition of only a single sulfur dioxide to either of the species examined by the Fackler group.

We have qualitative evidence for the addition of other Lewis acids to **3**. Addition of an ethyl ether solution of silver trifluoroacetate to a dichloromethane solution of **3** produces an adduct as seen by a new absorption in the electronic spectrum at 543 nm and the loss of the characteristic absorption of **3** at 508 nm. Likewise, addition of a dichloromethane solution of [Hg((CH<sub>3</sub>)<sub>2</sub>SO)<sub>6</sub>][O<sub>3</sub>SCF<sub>3</sub>]<sub>2</sub> to **3** in dichloromethane produces a new absorption at 556 nm. We suspect that these adducts form by the addition of the Lewis acid to one of the iridium centers in **3**. Extensive attempts to isolate these adducts in crystalline form suitable for X-ray diffraction have been unsuccessful.

The inability of the tin(II) adduct **4** to form a sulfur dioxide adduct may result from stronger Sn-Ir bonding (relative to the

(9) Balch, A. L.; Tulyathan, B. *Inorg. Chem.* **1977**, *16*, 2840.

(10) Wang, H.-H.; Pignolet, L. H.; Reedy, P. E., Jr.; Olmstead, M. M.; Balch, A. L. *Inorg. Chem.* **1987**, *26*, 377.

(11) King, C.; Heinrich, D. D.; Garzon, H. G.; Wang, J.-C.; Fackler, J. P., Jr. *J. Am. Chem. Soc.* **1989**, *111*, 2300.

**Table IV.** Atomic Coordinates ( $\times 10^4$ ) and Isotropic Thermal Parameters ( $\text{\AA}^2 \times 10^3$ ) for  $[\text{Ir}_2\text{Au}(\text{SO}_2)(\text{CO})_2\text{Cl}_2(\mu\text{-dpma})_2][\text{HSO}_4]$ 

	<i>x</i>	<i>y</i>	<i>z</i>	<i>U</i>		<i>x</i>	<i>y</i>	<i>z</i>	<i>U</i>
Ir(1)	4478 (1)	2224 (1)	464 (1)	23 (1) <sup>a</sup>	C(31)	-145 (19)	979 (21)	5357 (11)	121 (14) <sup>a</sup>
Ir(2)	3719 (1)	236 (1)	3352 (1)	33 (1) <sup>a</sup>	C(32)	290 (21)	632 (15)	5889 (10)	88 (10) <sup>a</sup>
Au	4416 (1)	1485 (1)	2022 (1)	23 (1) <sup>a</sup>	C(33)	1476 (21)	498 (17)	5783 (9)	94 (11) <sup>a</sup>
As(1)	2734 (1)	2383 (1)	2228 (1)	25 (1) <sup>a</sup>	C(34)	2147 (16)	767 (13)	5095 (8)	69 (8) <sup>a</sup>
As(2)	5914 (1)	423 (1)	1736 (1)	27 (1) <sup>a</sup>	C(35)	7231 (10)	1827 (8)	-522 (6)	27 (4) <sup>a</sup>
P(1)	2537 (3)	2595 (2)	708 (2)	23 (1) <sup>a</sup>	C(36)	7206 (13)	1192 (8)	-896 (7)	38 (5) <sup>a</sup>
P(2)	2638 (3)	1436 (2)	3711 (2)	32 (1) <sup>a</sup>	C(37)	7843 (13)	1259 (10)	-1571 (7)	48 (6) <sup>a</sup>
P(3)	4689 (3)	-995 (2)	2974 (2)	33 (1) <sup>a</sup>	C(38)	8493 (12)	1963 (10)	-1889 (7)	43 (5) <sup>a</sup>
P(4)	6359 (3)	1721 (2)	356 (2)	23 (1) <sup>a</sup>	C(39)	8549 (11)	2567 (9)	-1505 (7)	37 (5) <sup>a</sup>
Cl(1)	3967 (3)	755 (2)	724 (2)	30 (1) <sup>a</sup>	C(40)	7939 (10)	2517 (8)	-850 (7)	29 (4) <sup>a</sup>
Cl(2)	2391 (3)	69 (2)	2769 (2)	39 (1) <sup>a</sup>	C(41)	7095 (10)	2232 (8)	802 (7)	28 (4) <sup>a</sup>
S(1)	4741 (3)	2383 (2)	-821 (2)	36 (1) <sup>a</sup>	C(42)	8235 (10)	2075 (9)	722 (7)	35 (5) <sup>a</sup>
O(1)	5224 (8)	4045 (6)	163 (5)	41 (4) <sup>a</sup>	C(43)	8776 (12)	2416 (11)	1078 (7)	45 (6) <sup>a</sup>
O(2)	5329 (10)	388 (7)	4137 (5)	53 (5) <sup>a</sup>	C(44)	8217 (11)	2939 (10)	1524 (7)	42 (6) <sup>a</sup>
O(3)	3955 (9)	1817 (8)	-872 (5)	60 (5) <sup>a</sup>	C(45)	7061 (11)	3140 (9)	1614 (6)	33 (5) <sup>a</sup>
O(4)	4437 (14)	3317 (8)	-1063 (6)	81 (6) <sup>a</sup>	C(46)	6515 (10)	2780 (8)	1259 (6)	26 (4) <sup>a</sup>
C(1)	4894 (9)	3363 (8)	284 (6)	32 (5) <sup>a</sup>	C(47)	6524 (10)	556 (7)	723 (6)	23 (4) <sup>a</sup>
C(2)	4716 (12)	329 (9)	3839 (7)	37 (5) <sup>a</sup>	C(48)	7249 (11)	343 (9)	2037 (7)	37 (5) <sup>a</sup>
C(3)	1776 (10)	2125 (8)	261 (6)	26 (4) <sup>a</sup>	C(49)	7318 (13)	881 (10)	2472 (7)	43 (6) <sup>a</sup>
C(4)	1464 (9)	1259 (7)	464 (6)	23 (4) <sup>a</sup>	C(50)	8358 (15)	906 (12)	2629 (9)	59 (7) <sup>a</sup>
C(5)	903 (11)	921 (9)	108 (8)	40 (5) <sup>a</sup>	C(51)	9223 (13)	395 (12)	2369 (9)	64 (8) <sup>a</sup>
C(6)	642 (11)	1456 (11)	-493 (8)	46 (6) <sup>a</sup>	C(52)	9145 (13)	-165 (11)	1947 (8)	55 (6) <sup>a</sup>
C(7)	957 (11)	2271 (10)	-694 (8)	42 (6) <sup>a</sup>	C(53)	8154 (13)	-181 (11)	1763 (8)	51 (6) <sup>a</sup>
C(8)	1530 (10)	2622 (9)	-338 (7)	33 (5) <sup>a</sup>	C(54)	5331 (11)	-738 (8)	2027 (7)	33 (5) <sup>a</sup>
C(9)	2009 (10)	3727 (8)	579 (7)	30 (5) <sup>a</sup>	C(55)	3874 (11)	-1945 (9)	3093 (7)	37 (5) <sup>a</sup>
C(10)	2637 (12)	4356 (11)	51 (10)	59 (7) <sup>a</sup>	C(56)	2834 (16)	-2016 (11)	3555 (8)	61 (7) <sup>a</sup>
C(11)	2186 (18)	5214 (10)	-82 (11)	79 (10) <sup>a</sup>	C(57)	2267 (18)	-2751 (10)	3651 (9)	66 (8) <sup>a</sup>
C(12)	1095 (14)	5436 (10)	334 (11)	65 (9) <sup>a</sup>	C(58)	2734 (17)	-3405 (11)	3311 (9)	64 (8) <sup>a</sup>
C(13)	493 (15)	4800 (10)	825 (10)	63 (8) <sup>a</sup>	C(59)	3764 (16)	-3352 (10)	2861 (9)	57 (7) <sup>a</sup>
C(14)	938 (14)	3989 (10)	957 (9)	52 (7) <sup>a</sup>	C(60)	4337 (13)	-2623 (9)	2750 (7)	41 (6) <sup>a</sup>
C(15)	1896 (10)	2158 (8)	1631 (6)	29 (4) <sup>a</sup>	C(61)	5789 (14)	-1491 (9)	3387 (8)	45 (6) <sup>a</sup>
C(16)	2805 (10)	3617 (8)	2124 (7)	30 (5) <sup>a</sup>	C(62)	5516 (16)	-1663 (10)	4093 (8)	55 (7) <sup>a</sup>
C(17)	3804 (14)	3981 (9)	1878 (8)	52 (6) <sup>a</sup>	C(63)	6220 (16)	-2103 (12)	4454 (9)	67 (8) <sup>a</sup>
C(18)	3863 (14)	4886 (9)	1775 (8)	47 (6) <sup>a</sup>	C(64)	7263 (19)	-2381 (14)	4097 (11)	87 (11) <sup>a</sup>
C(19)	2954 (13)	5422 (10)	1877 (9)	51 (7) <sup>a</sup>	C(65)	7569 (17)	-2248 (14)	3367 (12)	84 (10) <sup>a</sup>
C(20)	1948 (16)	5053 (12)	2079 (15)	103 (13) <sup>a</sup>	C(66)	6798 (14)	-1782 (11)	3016 (8)	54 (7) <sup>a</sup>
C(21)	1855 (12)	4152 (11)	2222 (12)	73 (9) <sup>a</sup>	S(2)	8864 (4)	3012 (4)	3306 (3)	69 (2) <sup>a</sup>
C(22)	1732 (11)	1967 (10)	3156 (7)	38 (5) <sup>a</sup>	O(5)	9607 (10)	2777 (10)	2697 (7)	71 (6) <sup>a</sup>
C(23)	3346 (12)	2391 (8)	3754 (7)	35 (5) <sup>a</sup>	O(6)	9426 (12)	3354 (11)	3699 (7)	93 (7) <sup>a</sup>
C(24)	4492 (12)	2459 (9)	3465 (6)	35 (5) <sup>a</sup>	O(7)	8435 (15)	2058 (10)	3778 (8)	102 (8) <sup>a</sup>
C(25)	4961 (14)	3218 (10)	3475 (7)	49 (6) <sup>a</sup>	O(8)	7850 (12)	3492 (13)	3214 (9)	113 (9) <sup>a</sup>
C(26)	4341 (15)	3877 (11)	3746 (10)	61 (8) <sup>a</sup>	O(9)	3060 (9)	4201 (7)	-2042 (6)	53 (5) <sup>a</sup>
C(27)	3192 (16)	3788 (10)	4021 (8)	57 (7) <sup>a</sup>	S(3)	9708 (17)	4264 (13)	4647 (10)	82 (7)
C(28)	2674 (12)	3065 (10)	4019 (8)	43 (6) <sup>a</sup>	O(10)	10000	5000	5000	70
C(29)	1717 (13)	1153 (11)	4547 (7)	47 (6) <sup>a</sup>	O(11)	10182 (33)	3695 (25)	5105 (20)	65 (11)
C(30)	569 (18)	1256 (20)	4657 (10)	110 (13) <sup>a</sup>	O(12)	8681 (47)	4253 (36)	4718 (29)	108 (17)

<sup>a</sup> Equivalent isotropic *U* defined as one-third of the trace of the orthogonalized  $U_{ij}$  tensor.

Au–Ir bonding in **3**), which reduces the ability of the iridium centers to interact with an added Lewis acid. The Sn–Ir bond distances in **4** (2.741 (2), 2.742 (2) Å) are appreciably shorter than the Au–Ir distances (3.012 (1), 3.059 (1) Å) in **3**, and the tin is bound only to iridium (not to arsenic) in **4**.

### Experimental Section

**Preparation of Compounds.**  $\text{Ir}_2(\text{CO})_2\text{Cl}_2(\mu\text{-dpma})_2$ <sup>1a</sup> and  $[\text{Ir}_2\text{Au}(\text{CO})_2\text{Cl}_2(\mu\text{-dpma})_2]\text{Cl}^3$  were prepared as previously described.

**X-ray Crystallographic Studies.**  $\text{Ir}_2(\text{SO}_2)_2(\text{CO})_2\text{Cl}_2(\mu\text{-dpma})_2 \cdot 3\text{CHCl}_3 \cdot 0.5\text{CH}_2\text{Cl}_2$ . Yellow-green needles were obtained by saturating a dichloromethane/chloroform solution of **1** with sulfur dioxide and layering a sulfur dioxide solution of ethyl ether over this solution. The crystals grew at the initial solvent interface within 24 h. A suitable crystal was mounted on a glass fiber by using silicone grease and positioned in the cold stream of the X-ray diffractometer.<sup>12</sup> Only random fluctuations (<2%) in the intensities of two standard reflections were observed during the course of data collection. Crystal data are given in Table V.

The usual corrections for Lorentz and polarization effects were applied to the data. Crystallographic programs used were those of those of SHELXTL, version 5, installed on a Data General Eclipse computer.

Scattering factors and corrections for anomalous dispersion were from the ref 13.

The structure was solved by Patterson methods. An absorption correction was applied.<sup>14</sup> Two low-angle reflections suffering from extinction were omitted from the refinement. Final refinement was carried out with anisotropic thermal parameters for iridium, arsenic, chlorine, sulfur, and phosphorus atoms and isotropic parameters for carbon and oxygen. Hydrogen atoms were included at calculated positions by using a riding model with C–H of 0.96 Å and  $U_{\text{H}} = 1.2U_{\text{C}}$ . Two of the chloroform molecules and one dichloromethane were refined at half-occupancy. The largest shift in the final cycle of refinement was 0.018 for *y* of P(1). The largest peak in the final difference map was 2.1 e Å<sup>-3</sup>, 1.27 Å from a chlorine atom of a disordered chloroform molecule.

$[\text{Ir}_2\text{Au}(\text{SO}_2)_2(\text{CO})_2\text{Cl}_2(\mu\text{-dpma})_2][\text{HSO}_4] \cdot 0.32\text{SO}_2 \cdot 1.23\text{H}_2\text{O}$ . A suitable crystal was obtained by saturating a dry, degassed dichloromethane solution of **3** with sulfur dioxide and placing a layer of sulfur dioxide saturated ethyl ether over it. The tube containing this mixture was placed in a freezer at -20 °C and stored there for 6 weeks. The tube was sealed with a serum cap, but leakage through this was a likely source of oxygen and moisture. Moreover, the crystal growing tube was not oven-dried and represents another source of moisture. The crystal was then transferred to the diffractometer as described previously. Other similar but

(12) Hope, H. In *Experimental Organometallic Chemistry: A Practicum in Synthesis and Characterization*; Wanda, A. L., Darenbourg, M. Y., Eds.; ACS Symposium Series 357; American Chemical Society: Washington, DC, 1987; Chapter 10.

(13) *International Tables for X-ray Crystallography*; Kynoch: Birmingham, England, 1974; Vol. 4.

(14) The method obtains an empirical absorption tensor from an expression relating  $F_o$  and  $F_c$ ; Moezz, B. Ph.D. Thesis, University of California, Davis, CA, 1987.

**Table V.** Crystal Data and Data Collection Solution, and Refinement Parameters for  $\text{Ir}_2(\text{SO}_2)_2(\text{CO})_2\text{Cl}_2(\mu\text{-dpma})_2 \cdot 3\text{CHCl}_3 \cdot 0.5\text{CH}_2\text{Cl}_2$  (**5**) and  $[\text{Ir}_2\text{Au}(\text{SO}_2)(\text{CO})_2\text{Cl}_2(\mu\text{-dpma})_2][\text{HSO}_4] \cdot 0.32\text{SO}_2 \cdot 1.23\text{H}_2\text{O}$  (**6**)

	5	6
formula	$\text{C}_{68}\text{H}_{60}\text{As}_2\text{Cl}_2\text{-Ir}_2\text{O}_6\text{P}_4\text{S}_2$	$\text{C}_{66}\text{H}_{61.5}\text{AuAs}_2\text{Cl}_2\text{-Ir}_2\text{O}_{9.9}\text{P}_4\text{S}_{2.3}$
fw	2120.9	2012.92
color and habit	yellow green needles	red prisms
cryst syst	monoclinic	triclinic
space group	$P2_1/n$ (No. 14)	$P1$
<i>a</i> , Å	14.699 (4)	12.548 (4)
<i>b</i> , Å	15.351 (6)	15.721 (4)
<i>c</i> , Å	38.026 (10)	20.556 (5)
$\alpha$ , deg		76.97 (2)
$\beta$ , deg	100.03 (3)	73.60 (2)
$\gamma$ , deg		83.35 (2)
<i>V</i> , Å <sup>3</sup>	8449 (5)	3784 (2)
<i>T</i> , K	130	130
<i>Z</i>	4	2
<i>d</i> <sub>calcd</sub> , g cm <sup>-3</sup> (130 K)	1.67	1.77
radiation Å	Mo K $\alpha$ ( $\lambda = 0.71069$ Å)	Mo K $\alpha$ ( $\lambda = 0.71069$ Å)
$\mu$ (Mo K $\alpha$ ), cm <sup>-1</sup>	46.6	67.7
range of transmissn factors	0.51-0.63	0.27-0.48
cryst dimens, mm	0.12 $\times$ 0.13 $\times$ 0.27	0.13 $\times$ 0.20 $\times$ 0.37
<i>R</i> <sup>a</sup>	0.078	0.059
<i>R</i> <sub>w</sub> <sup>a</sup> [ <i>w</i> = 1/( $\sigma^2(F_o)$ )]	0.079	0.065

$$^a R = \sum ||F_o| - |F_c|| / |F_o|, \text{ and } R_w = \sum ||F_o| - |F_c|| w^{1/2} / \sum |F_o w^{1/2}|.$$

smaller crystals were used to collect the infrared data. However, the yield of crystals was low. Crystal data and data collection parameters are given in Table V and in the supplementary material. Data analysis and refinement follow the procedure outlined above. Two low-angle reflec-

tions that were affected by extinction were removed from the data. One site in the structure is shared by a molecule of water and a molecule of SO<sub>2</sub>. Two models were devised and compared. A group occupancy for the SO<sub>2</sub> molecule refined to 0.313 (9). The thermal parameter of the oxygen of the water molecule (O(10)) at the center of symmetry was fixed at 0.07 Å<sup>2</sup> and the occupancy allowed to refine. It converged at 0.23 (2). In the alternative model to eliminate a suspicious S...S contact at 3.25 Å, the water oxygen occupancy was reset to 0.5 minus the group occupancy of the SO<sub>2</sub> group and refined; the thermal parameters were kept free. This yielded an occupancy of 0.34 (1) for the SO<sub>2</sub> and 0.16 (1) for the water. The water oxygen thermal parameter in this case refined to 0.03 (1) Å<sup>2</sup> while the SO<sub>2</sub> thermal parameters were essentially unchanged. The two models appear satisfactorily similar. The data reported come from the first model. In the last cycles of refinement all non-hydrogen atoms except the disordered SO<sub>2</sub> and water oxygen were assigned anisotropic thermal parameters. In the final difference map the largest feature was 3.1 e Å<sup>-3</sup> in height, 0.94 Å from Au. Several remaining peaks were also large, but were in the vicinity of heavy atoms and not of any chemical significance.

There are two O...O distances that are indicative of hydrogen bonding, O(4)...O(9)/3.02 (1) Å, and O(6)...O(12) = 2.68 (7) Å. The first corresponds to one of the oxygens of the terminally bound SO<sub>2</sub> and a molecule of H<sub>2</sub>O; the second corresponds to one of the HSO<sub>4</sub><sup>-</sup> oxygens and one of the partially occupied SO<sub>2</sub> oxygens. However, definitive crystallographic identification of the anion as bisulfate (rather than sulfate) was not possible.

**Acknowledgment.** We thank the National Science Foundation (Grant CHE 8519557) for support and Johnson Matthey, Inc., for a loan of iridium salts.

**Supplementary Material Available:** Tables of crystal data and structural determination parameters, bond distances, bond angles, anisotropic thermal parameters, and hydrogen atom positions for **4** and **5** (15 pages); listings of observed and calculated structure factors (85 pages). Ordering information is given on any current masthead page.

Contribution from the Department of Chemistry, University of British Columbia, 2036 Main Mall, Vancouver, British Columbia V6T 1Y6, Canada

## Aluminum and Gallium Complexes of 1-Ethyl-3-hydroxy-2-methyl-4-pyridinone: A New Exoclathrate Matrix

William O. Nelson, Steven J. Rettig, and Chris Orvig\*

Received February 22, 1989

1-Ethyl-3-hydroxy-2-methyl-4-pyridinone and its aluminum(III) and gallium(III) complexes have been prepared and characterized; all three compounds have been studied by single-crystal X-ray diffraction. The uncomplexed ligand C<sub>8</sub>H<sub>11</sub>NO<sub>2</sub> (HL) crystallized in the orthorhombic space group *Pbca* with following the crystal parameters: *a* = 12.5907 (8) Å, *b* = 11.7477 (6) Å, *c* = 11.0040 (6) Å, *Z* = 8. The complexes M(C<sub>8</sub>H<sub>10</sub>NO<sub>2</sub>)<sub>3</sub>·12H<sub>2</sub>O (ML<sub>3</sub>·12H<sub>2</sub>O) are isostructural for M = Al and Ga, crystallizing in the trigonal space group *P3* with following the crystal parameters for Al (Ga): *a* = 17.1734 (8) Å, (17.247 (1) Å), *c* = 6.827 (1) Å (6.830 (2) Å), *Z* = 2. For the three compounds HL, AlL<sub>3</sub>·12H<sub>2</sub>O, and GaL<sub>3</sub>·12H<sub>2</sub>O, respectively, the data were refined by using 1228, 1157, and 1918 reflections with *I* ≥ 3[ $\sigma(I)$ ] to *R* values of 0.053, 0.032, and 0.029 and *R*<sub>w</sub> values of 0.085, 0.038, and 0.036. The two metal complexes form rigidly *fac* geometries with extensive hydrogen bonding to channels of water molecules involving every available oxygen atom in the unit cell. This structure is an exoclathrate. The Al and Ga complexes show "tucked away" ethyl units that allow the structural integrity of the exoclathrate lattice (including the water channels) to be maintained. On comparison of six exoclathrate crystal structures, a trend was noticed toward deformation of the metal complex rather than the hexagonal channels of water molecules in order to accommodate changes in metal ion or N substituent.

The recent discovery of the exoclathrate lattice, which incorporates hexagonal channels of water molecules hydrogen bonded to tris(3-hydroxy-1,2-dimethyl-4-pyridinonato)metal(III) units (metal = Al<sup>1,2</sup>, Ga,<sup>2</sup> In,<sup>3</sup> Fe<sup>4</sup>), has prompted a search for other examples of this complex binding array. Through variation of the substituent on the ring nitrogen atom, this search is being undertaken in metal/ligand systems that are closely related to those in which the lattice was first discovered.

In an effort to study the limitations of the exoclathrate lattice, we have replaced the *N*-methyl group of the ligand with an *N*-ethyl substituent; we report here the Al and Ga complexes of 1-

\* To whom correspondence should be addressed.

- (1) Nelson, W. O.; Rettig, S. J.; Orvig, C. *J. Am. Chem. Soc.* **1987**, *109*, 4121.
- (2) Nelson, W. O.; Karpishin, T. B.; Rettig, S. J.; Orvig, C. *Inorg. Chem.* **1988**, *27*, 1045.
- (3) Matsuba, C. A.; Nelson, W. O.; Rettig, S. J.; Orvig, C. *Inorg. Chem.* **1988**, *27*, 3935.
- (4) Charalambous, J.; Dodd, A.; McPartlin, M.; Matondo, S. O. C.; Pattrana, N. D.; Powell, H. R. *Polyhedron* **1988**, *7*, 2235.